Published in final edited form as:
Neuroimage. 2011 February 1; 54(3): 1942–1950. doi:10.1016/j.neuroimage.2010.09.079.

Reducing the Gradient Artefact in Simultaneous EEG-fMRI by Adjusting the Subject's Axial Position

Karen J. Mullinger, **Winston X. Yan**, and **Richard Bowtell**
Sir Peter Mansfield Magnetic Resonance Centre, School of Physics and Astronomy, University of Nottingham, University Park, Nottingham, NG7 2RD, UK.

Abstract

Large artefacts which compromise EEG data quality are generated when electroencephalography (EEG) and functional magnetic resonance imaging (fMRI) are carried out concurrently. The gradient artefact produced by the time-varying magnetic field gradients is the largest of these artefacts. Although average artefact correction (AAS) and related techniques can remove the majority of this artefact, the need to avoid amplifier saturation necessitates the use of a large dynamic range and strong low-pass filtering in EEG recording. Any intrinsic reduction in the gradient artefact amplitude would allow data with a higher bandwidth to be acquired without amplifier saturation, thus increasing the frequency range of neuronal activity that can be investigated using combined EEG-fMRI. Furthermore, gradient artefact correction methods assume a constant artefact morphology over time, so their performance is compromised by subject movement. Since the resulting, residual gradient artefacts can easily swamp signals from brain activity, any reduction in their amplitude would be highly advantageous for simultaneous EEG-fMRI studies. The aim of this work was to investigate whether adjustment of the subject's axial position in the MRI scanner can reduce the amplitude of the induced gradient artefact, before and after artefact correction using AAS. The variation in gradient artefact amplitude as a function of the subject's axial position was first investigated in six subjects by applying gradient pulses along the three Cartesian axes. The results of this study showed that a significant reduction in the gradient artefact magnitude can be achieved by shifting the subject axially by 4 cm towards the feet relative to the standard subject position (nasion at iso-centre). In a further study, the 4 cm shift was shown to produce a 40% reduction in the RMS amplitude (and a 31% reduction in the range) of the gradient artefact generated during the execution of a standard multi-slice, EPI sequence. By picking out signals occurring at harmonics of the slice acquisition frequency, it was also shown that the 4 cm shift led to a 36% reduction in the residual gradient artefact after AAS. Functional and anatomical MR data quality is not affected by the 4 cm shift, as the head remains in the homogeneous region of the static magnet field and gradients.

Keywords

Simultaneous EEG-fMRI; gradient artefact; subject positioning; artefact reduction; high frequency EEG

Address for Correspondence: Professor Richard Bowtell, Sir Peter Mansfield Magnetic Resonance Centre, School of Physics and Astronomy, University of Nottingham Nottingham NG7 2RD UK richard.bowtell@nottingham.ac.uk Tel: +44 115 9514737 Fax: +44 115 9515166.

Europe PMC Funders Author Manuscripts

Introduction

Simultaneous electroencephalography (EEG) and functional Magnetic Resonance Imaging (fMRI) has become a widely used technique for studying brain activity. Applications of this technique are now far reaching, ranging from the study of brain networks associated with the resting state (Laufs et al. 2003) to the investigation of epileptic foci (Iannetti et al. 2002; Laufs et al. 2007; Lemieux 2004; Salek-Haddadi et al. 2002; 2003). Concurrent EEG-fMRI has also been extensively used to investigate the relationship between BOLD signal changes and evoked potentials (Debener et al. 2006; Eichele et al. 2005; Mobascher et al. 2009; Schubert et al. 2008; Strobel et al. 2008; Warbrick et al. 2009). The successful exploitation of the combined EEG-fMRI technique is remarkable given the very large artefacts that are generated in EEG data recorded during concurrent fMRI. The main confounding factors are the pulse artefact caused by pulsatile motion linked to the cardiac cycle (Allen et al. 1998; Debener et al. 2008; Ives et al. 1993; Yan et al. 2010) and the gradient artefact produced by the temporally varying magnetic fields required for MR imaging (Allen et al. 2000). Both of these artefacts are generally orders of magnitude larger than the neuronal activity of interest, but their inherent periodicity and known or measurable timings facilitate artefact correction by post-processing techniques, such as average artefact subtraction (AAS) (Allen et al. 2000; Allen et al. 1998). It is these techniques which underpin the successful implementation of combined EEG-fMRI.

Nevertheless, the contamination of raw EEG recordings made during continuous fMRI by artefact voltages that are many times larger than the signals of interest does pose a number of limitations on concurrent EEG recordings. These include the requirements for a large dynamic range and limited bandwidth. The disparity in the magnitude of the artefacts and signal of interest also means that very high performance in artefact correction is required, since a residual artefact can still completely swamp the neuronal signals, even if highly attenuated compared with the artefacts appearing in the uncorrected data. In this work, we focus on the gradient artefact, which is generally at least an order of magnitude larger than the pulse artefact, and describe a simple method, involving adjustment of the axial position of the subject, that can be used to reduce the amplitude of this artefact in the recorded data.

Use of the average artefact subtraction (AAS) technique, developed by Allen and coworkers (Allen et al. 2000), to perform gradient artefact correction involves forming an average gradient artefact template and then subtracting this template from each occurrence of the gradient artefact in the EEG data. This requires accurate sampling of the gradient artefact waveform, which means that the artefact must be precisely sampled and smaller in magnitude than the dynamic range of the EEG system. The former requirement can be achieved through synchronisation of the MR scanner and EEG clocks (Mandelkow et al. 2006; Mullinger et al. 2008a), while the latter requires the use of an EEG system with a very high dynamic range and/or limiting of the amplitude of the gradient artefact.

The magnitude of the gradient artefact voltage depends on the rate of change of magnetic flux linked by loops effectively formed by the EEG leads and the conducting tissues of the head. To make an approximate estimate of the size of the gradient artefact we assume an easily generated, average rate of change of magnetic field in the head of 20 T s^{-1} and an effective loop area of 50 cm^2. This yields an induced voltage of 100 mV, which is more than 10,000 times larger than a typical evoked response in an EEG recording. Accurate recording of EEG signals in the presence of such large artefact voltages would require a very large dynamic range and a large number of bits in signal digitisation. Fortunately the power spectrum of the gradient artefacts is dominated by contributions that are much higher in frequency than the signals of most common interest in EEG recordings. This means that low-pass filtering can be used to reduce the gradient artefact voltages to a more manageable

level in EEG recordings made during concurrent MRI without corrupting the EEG data. Hardware filtering of the voltages at the EEG amplifiers' inputs is usually therefore applied and with a typical cut-off frequency of 250 Hz the peak artefact voltage can be reduced by more than a factor ten, thereby reducing the dynamic range required to avoid amplifier saturation. With this level of filtering it is still possible for typical gradient waveforms to cause amplifier saturation and further increases in the performance of the gradient systems used in MRI scanners will exacerbate this problem. Recording with a higher bandwidth provides benefits by allowing more accurate sampling of the rapidly varying gradient artefacts and is a necessity for those interested in measuring ultra-high frequency signals from the brain in combined EEG-fMRI experiments (Freyer et al. 2009). EEG systems incorporating hardware filters with a cut-of frequency of 1 kHz and higher are available, but they are more prone to saturation by the larger resulting gradient artefact voltages. In light of the above discussion it can be seen that a reduction of the amplitude of the gradient artefact voltages produced during concurrent EEG/fMRI would be of significant value since it would allow a relaxation of the constraints on dynamic range and bandwidth that could be usefully exploited in many studies.

A further problem with the implementation of AAS and other techniques for gradient artefact correction arises when subject movement occurs during a study. Changes in subject position alter the morphology of the induced gradient artefacts, meaning that the artefact voltage waveforms recorded at each electrode vary over volume acquisitions. As a consequence residual artefacts remain after AAS, since the average artefact template does not exactly characterise individual occurrences of the gradient artefact. This problem is often partially resolved by using a sliding time-window to form the average artefact template (Allen et al. 2000); Becker et al. 2005). Moosmann *et al* (Moosmann et al. 2009) have recently taken this concept further, by using information about the occurrence of subject movements derived from the MRI realignment parameters, to guide the formation of templates, while Freyer et al. (Freyer et al. 2009) analysed the similarity of the artefact produced by a particular image acquisition to the artefacts generated during all other image acquisitions, and then formed a varying correction template by weighted summation over a limited number of the most similar artefact waveforms.

Although these methods can improve the efficacy of artefact removal, the reduced number of repeated artefact waveforms which they may use in forming correction templates means that there is a greater risk that signals due to neuronal activity will be attenuated in the correction process (Mullinger et al. 2008b). Other sources of temporal instability in the generation or sampling of the gradient artefact voltages, including scanner timing errors and lack of synchronisation of the EEG sampling and gradient waveforms (Mandelkow et al. 2006; Mullinger et al. 2008a) also lead to partial failure of AAS. The large residual artefacts that arise as a consequence of this failure can easily overwhelm the signals of interest from the brain. Further digital filtering of the EEG data after artefact correction with AAS is therefore regularly employed to address this issue. This application of additional low-pass filtering, with a low frequency cut-off that is often less than 80 Hz (Allen et al. 2000; Benar et al. 2007; Comi et al. 2005; Ertl et al. 2010; Gebhardt et al. 2008; Mayhew et al. 2010), restricts the range of brain signals that can be investigated in concurrent EEG-fMRI experiments. In particular, residual gradient artefacts can make recording activity across the gamma band (30-100 Hz) problematic in combined EEG-fMRI experiments (Ryali et al. 2009), while recording of ultra-high frequency activity currently requires interleaving of EEG and MRI data acquisition. Such interleaving can be achieved by using the stepping stone approach (Anami et al. 2003), but this requires non-standard modification of the imaging sequence used for fMRI data acquisition. Any steps that would reduce the intrinsic sensitivity to these residual gradient artefacts would therefore be highly beneficial for combined EEG-fMRI studies.

In recent work, we showed how the pattern of gradient artefacts induced on different leads by time-varying longitudinal and transverse gradients could be modelled analytically and numerically (Yan et al. 2009) based on knowledge of the lead paths and head position in the gradient fields. This modelling work provided some insight into ways in which the magnitude of the gradient artefact could be reduced. In particular, the models suggested that adjustment of the axial position of the subject's head in the scanner could reduce the overall amplitude of the gradient artefact. In essence this involves positioning the subject so that the maximum rate of change of magnetic field produced by the time-varying gradients over the EEG leads is minimised. In the previous work (Yan et al. 2009) we partially confirmed the prediction of the simulations by measuring the gradient artefacts at two different axial positions, but did not explore in any detail the benefits of subject repositioning for combined EEG-fMRI studies.

The aim of the study described here is therefore to measure the effects of the subject's axial position on the characteristics of the gradient artefacts, and to assess the effect of optimal positioning on the residual artefact after AAS has been applied to data recorded during concurrent fMRI. The first part of the study focused on finding the axial position at which optimal reduction of the artefacts due to *x*-, *y*- and *z*- gradients is produced. This involved implementing a customised pulse sequence in which controlled gradient pulses were sequentially applied along the three Cartesian axes. In the second part of the study, we tested whether the gradient artefacts were reduced by adopting the optimal subject position in a typical EEG-fMRI experiment. We compared the gradient artefacts generated by a multi-slice EPI sequence (as used in the vast majority of fMRI experiments) when the subject was in the optimal axial position identified in the first part of the study, to recordings made with standard subject positioning (nasion at iso-centre). We also investigated whether the artefacts that remained after AAS were reduced when the subject was moved to the optimal axial position. Finally we tested whether shifting the subject to the optimal axial position had any effect on the quality of MRI data.

Methods

EEG data were recorded using a 32-electrode EEG cap (Brain Products, Munich, Germany) with 31 electrodes following the extended international 10-20 system and a reference electrode positioned at FCz. This cap had an additional channel for electrooculography (EOG) which was attached beneath the left eye. A BrainAmp MR-plus EEG amplifier (Brain Products, Munich, Germany) with Vision Recorder (Version 1.10) was used for recording data in a Philips Achieva 3 T MR scanner (Philips Medical Systems, Best, Netherlands). The EEG clock was synchronised to the MR scanner clock for all experiments to ensure consistent sampling of the waveforms (Mandelkow et al. 2006).

A 1-m-long ribbon cable running axially along the magnet bore was used to connect the EEG amplifier to the cap. The EEG amplifier was placed just outside the bore of the magnet on a table, which isolated it from vibrations of the scanner. The ribbon cable was held in tension and suspended above the mounting for the scanner bed, thus also decoupling the cable from scanner vibrations (Mullinger et al. 2008c). We tried to keep the cable path the same for recordings made at different axial positions, so as to limit variation of the voltages induced in the cable (Yan et al. 2009). For each study, six subjects, from a cohort of eight volunteers (four male), were scanned with approval of the local ethics committee and informed consent.

Study 1

In order to assess how axial repositioning of the subject affected the magnitude of the gradient artefact produced by each of the three orthogonal gradients, EEG recordings were

made during execution of a modified EPI sequence. This incorporated three additional gradient pulses applied sequentially in the Anterior-Posterior (AP), Right-Left (RL) and Foot-Head (FH) directions prior to each slice acquisition, as shown in Fig. 1. Each trapezoidal pulse was made up of two ramps of 10 ms, during which the gradient changed at a rate of 2 T $m^{-1}s^{-1}$, and a 10 ms period during which the gradient remained constant. A 20 ms gap was inserted between successive gradient pulses. The modified sequence provided clearly-defined periods during which just a single gradient varied in time in a well defined manner. This allowed easy separation of the effects of the three different gradients. This is in contrast to the situation during the EPI acquisition when time-varying gradients are simultaneously applied along multiple axes, often varying at high frequencies such that the EEG system's low-pass filtering significantly attenuates and temporally smears the induced voltages, therefore making it difficult to differentiate the voltages produced by individual gradient pulses and thus to quantify the effect of a time-varying gradient applied along one particular direction.

Recordings were made with the subject located at 15 different axial positions. Subject position was defined by the z-co-ordinate of the nasion with zero defined to correspond to alignment of the nasion with the scanner's iso-centre. For all recordings, the subject's head was centred with respect to the scanner's left-right axis and at a fixed position in the anterior-posterior direction. Axial position was varied from −4 cm to +10 cm in 1 cm steps, with positive values corresponding to an axial shift towards the feet. Artefacts from thirty pulses applied along the three gradient axes were recorded at each position with a sampling rate of 5 kHz. Filters which limit the frequency range of the recorded signals were set to 0.016-1000 Hz, with a roll-off of 30 dB/octave at high frequency.

Some further measurements were made in order to ascertain the variation of head size across subjects in the study. An anatomical image was acquired with the subject positioned at iso-centre using a standard MPRAGE sequence (Mugler et al. 1990) with 1 mm isotropic resolution. Head dimensions for each individual were established from these data by measuring the distance between the ears (dRL), from the nasion to the back of the head (dAP) and from the top of the head perpendicular to the intercept of the dAP and dRL lines (dHF). The distance from the nasion to the line joining the Fp1 and Fp2 electrodes was also measured manually on the surface of the scalp on each subject.

EEG data analysis was carried out using Brian Vision Analyzer2 (Version 2.0.1.3417, Brain Products GmbH, Munich, Germany) and Matlab. As shown in Fig. 1, each gradient pulse commenced with a 10 ms period during which the rate of change of gradient, $\dot{G}$, is constant and positive, followed 10 ms later by a 10 ms period in which $\dot{G}$ is constant and negative. Equal and opposite artefact voltages are thus generated during the two ramping periods. To form a robust measure of the artefact voltage on each electrode the gradient artefact was averaged over the 30 pulses (Fig 1), and we then evaluated the average voltage over the central 5 ms of each ramp period, before taking the difference between the two values. This eliminated the effect of any baseline offset and high frequency fluctuations. The change in the severity of the gradient artefact with the subject's axial position was characterised by calculating the range and the root-mean-square amplitude (RMS) of the artefact voltage across the 31 electrodes located on the head and then averaging these measures over subjects.

Study 2

To evaluate the effect of axial head position on the gradient artefact generated in typical fMRI studies, EEG data were recorded over an 8 minute period whilst a standard axial, multi-slice EPI sequence (TR = 2.5 s, TE = 40 ms, 96×96 matrix, 3×3 mm^2 in-plane resolution, flip angle = 85°, SENSE factor = 2 - i.e. a twofold reduction in the number of

phase encode lines of k-space acquired - and 4 mm slice thickness) was executed. Thirty two transverse slices were acquired with equidistant temporal spacing in each TR period, so that the frequency of slice acquisition was 12.8 Hz. This imaging sequence provided whole-brain coverage, which allowed realignment parameters to be calculated using SPM5 (FIL, London, http://www.fil.ion.ucl.ac.uk/spm/software/spm5/). The amount of head movement during each recording could thus be assessed. Experiments were carried out with the subjects: (i) positioned with their nasion at iso-centre and (ii) positioned at the optimal axial offset identified in Study 1. For this second study, the filters which limit the frequency range at which the EEG data were recorded were set to 0.016-250 Hz. This bandwidth is more typical of that used in current EEG-fMRI experiments and its use here was necessary to avoid saturation of the EEG amplifiers due to the large gradient artefacts produced when the subjects were positioned with nasion at iso-centre.

To allow assessment of the effect of axial positioning on the variation of artefact magnitude due to movement during image acquisition, subjects were cued to move both feet via plantar/dorsal ankle flexion for 5 s every 30 s during the recording. This foot movement was found to generate cumulative head movements of less than 1 mm in amplitude, thus mimicking positional changes which may occur naturally during longer fMRI studies. Subjects were asked to move their feet in a similar manner during the recordings made at the two axial positions and the order of recording at the different positions was randomised across subjects.

In one subject, we also acquired anatomical images (1 mm isotropic resolution) at the two axial positions, in order to evaluate any effect of the 4 cm shift. In a single session, the subject was scanned at the 0 cm position, then with the 4 cm shift and then again at the 0 cm position.

Analysis of gradient artefacts was carried out in Matlab both before and after gradient artefact correction using AAS. The artefact template used for correction spanned one TR period and was formed by averaging over the entire eight-minute acquisition. Use of this long averaging period ensured maximum sensitivity to changes in the gradient artefact due to motion. Data were not down-sampled or subjected to further low-pass filtering so as to allow gradient artefact signals to be assessed across the entire 0.016-250 Hz frequency band.

The effect of subject repositioning on the strength of the gradient artefacts produced by the multi-slice EPI sequence was evaluated using a number of different measures. To assess the effect of the optimal position on the gradient artefacts prior to correction, the artefact voltage waveform produced on each lead during the acquisition of each slice was averaged over slice acquisitions (excluding segments where the cued motion occurred, so as to avoid contamination of the signals with any voltages produced by movement in the strong magnetic field(Yan et al. 2010)) and the RMS-voltage over the 78 ms duration of the average “slice” artefact was then calculated and averaged across leads and subjects. In order to evaluate the effect of subject position on the residual gradient artefact after AAS we also calculated the variance across equivalent time points in multiple slice acquisitions for each lead and then averaged across leads and subjects; data acquired during periods of movement were again excluded from this calculation. A further measure of the effect of repositioning on the residual gradient artefact was obtained by studying the harmonics of the slice frequency. The attenuation produced by the 4 cm shift at the first ten harmonics of the slice frequency was found by initially taking the Fourier transform of the whole recordings on each lead at the two positions. The attenuation in dB of the power at the optimal relative to isocentre position for each of the slice harmonic frequencies was then measured. An average of the attenuation over all leads and subjects was then found.

To test whether head movements at the two positions were similar across subjects the RMS of the mean-corrected realignment parameters (x, y and z translation, and pitch, yaw and roll) were found for both data sets. A Wilcoxon signed-rank test was then performed for each realignment parameter to compare the motion that occurred at the two different positions.

Two different analyses were used to assess the effect of the subject repositioning on the MRI data. First, we compared the temporal signal-to-noise-ratio (SNR) of the EPI data recorded at the two positions. To do this, the data were first motion corrected and then subjected to high-pass filtering with a cut-off frequency of 0.033 Hz in order to remove the effects of scanner drift and other slow signal variation. The SNR of the data was then assessed by pixel-wise calculation of the ratio of the mean to the temporal standard deviation. This ratio was averaged over a region of interest (ROI) made up of about 625 voxels in the visual cortex. Second, we co-registered the three different anatomical images using SPM5 and then compared the difference images formed by subtracting the images acquired at the 0 and 4 cm positions, with those produced by subtracting the two images acquired at the 0 cm position.

Results

Subjects exhibited little variation in head dimensions with dRL = 15.5 ± 0.8 cm and dAP = 19 ± 1 cm (average ± standard deviation across subjects). There was a slightly greater variation in the measure of size in the foot-head direction, dFH = 10 ± 4 cm, and in the distance from the nasion to the frontal electrodes = 7 ± 2 cm.

Study 1

Figure 2A and B show the variation with axial position of the RMS and range over electrodes of the artefact voltages produced by time-varying gradients applied along the three Cartesian axes. The plotted values are averaged over the six subjects studied and the error bars show the standard deviation over subjects.

These plots show that moving the subject axially produces a significant variation of the magnitude of the gradient artefact produced by the three different gradients and that there is an axial position at which the range and RMS of the artefact voltages produced by each of the gradients is minimised. In the case of the RL and FH gradients, the average RMS and range of the gradient artefact voltage are significantly reduced by axially repositioning the subject so that the nasion is shifted away from iso-centre towards the feet by 4 - 6 cm. However in the case of the AP gradient the minimum in the RMS and range occurs for axial offsets in the 0 – 2 cm range, such that there is no significant reduction in the artefact voltage compared with that measured with the nasion at iso-centre.

Analysis of these plots indicates that axially shifting the subject by 4 cm towards the feet provides a sensible compromise between the competing effects in reducing the overall gradient artefact magnitude. At this position, the RMS of the gradient artefact across electrodes is decreased by 50, 42 and 5% for the RL, FH and AP gradients, respectively, and the range of the gradient artefact amplitude across electrodes is decreased by 43% and 39% for the RL and FH gradients whilst a 4% increase occurs for the AP gradient. An axial shift of 4 cm in the foot-direction was therefore used as the optimal subject position in Study 2.

Study 2

Figure 3 shows maps of the RMS value of the average gradient artefact over a typical fMRI slice acquisition with the subjects positioned with nasion at iso-centre (A) and at the optimal position corresponding to a shift of 4 cm in the direction of the feet (B), averaged over all

subjects. Figure 3C shows the difference of these two maps with the positive values indicating that the gradient artefact is smaller in magnitude at the optimal position. The greatest reduction occurs for posterior electrodes, although a significant decrease of ($p<0.01$ from a student t-test) the gradient artefact was found on all channels. When averaged over electrodes, the 4 cm axial displacement from iso-centre produced a 31% (40%) reduction in the range (RMS) of the gradient artefact. These results demonstrate that the reduction in the voltage generated by individual gradients after axial repositioning that was identified in Study 1, translates into a reduction of the gradient artefact generated in conventional multi-slice EPI acquisition, as used in most EEG-fMRI experiments.

This reduction is also evident from Fig. 4, which shows the variation of the RMS value of the average artefact across subjects and leads over a slice acquisition for the two positions (Fig. 4A). These plots were calculated by averaging the voltages on each lead over slice acquisitions and then finding the RMS value across leads at each time point, before averaging over subjects. The largest artefact voltages occur at times of 10-16 ms (resulting from the gradient pulses used in fat suppression and slice selection), 38-42 ms (due to the pre-excursion pulses at the start of the echo train) and 65-72 ms (resulting from the crusher gradients at the end of the echo train) and the tight band-pass filtering employed in this Study (0.0016 – 250 Hz) means that voltages due to the high-frequency, switched read gradient used in generating the EPI echo-train do not feature strongly in the plots. The reduction in the magnitude of the artefact produced by the axial repositioning is evident from a visual comparison of the two traces in Fig. 4A

The square root of the average variance across slices is also plotted as a function of time through the slice acquisition in Fig. 4B for the two different subject positions. It is obvious from inspection of these data that the greatest residual signal variation after correction occurs at times which are coincident with the appearance of the largest artefact voltages in the uncorrected recordings. Comparison of the two plots indicates that the residual artefacts at these times are smaller at the 4-cm-shifted position. However the plots of the average standard deviation after correction show a baseline offset of about 50 μV, resulting from other sources of variation in the EEG recordings including the pulse artefact, the effect of small head rotations in the strong, static magnetic field, as well as true brain signals. To provide a more quantitative measure of the effect of the subject's axial position on the residual gradient artefact, we also therefore carried out a Fourier analysis and then focused on signals occurring at harmonics of the 12.8 Hz slice frequency.

Figure 5 shows the attenuation of the AAS-corrected signal at the first ten harmonic frequencies, which was produced by the 4 cm shift. These data indicate that the power of the residual artefact is reduced at the +4 cm-subject position compared with that measured at iso-centre at all of the ten harmonic frequencies shown. The average attenuation across these harmonics is 4.4 ± 1.4 dB. The error bars show the standard deviation over subjects of the average attenuation over leads. These indicate that there is a significant variation in the level of attenuation measured in different subjects. A Wilcoxon signed-rank test indicated that only the attenuation of the first harmonic was significant ($p=0.046$) while the measured attenuation of the fourth, seventh, ninth and tenth harmonics approached significance ($p=0.075$). As a better measure of the effect of position optimisation on residual gradient artefacts we considered all harmonics of the slice frequency in the 0-250 Hz range of the hardware filtering. The entire datasets (including times when cued movement took place) were effectively filtered to include only a 0.2 Hz frequency range around each of the harmonics of the slice frequency: this was achieved by using a 4^{th} order band rejection filter in BrainVision Analyzer2 (Brain Products, Munich) and subtracting the filtered data from the original so only the harmonics remained. The RMS amplitudes of the resulting signals were then calculated and averaged over leads and subjects for the two different positions

yielding values of 18 ± 8 μV at iso-centre and 12 ± 4 μV at the optimal position. This 36 % reduction in overall RMS of the EEG signal at slice frequency harmonics was found to be significant across subjects when a Wilcoxon-signed rank test was performed.

The Wilcoxon signed-rank test that was used to assess whether subject movement was different in the recordings made at the two different positions showed no significant difference of any of the individual realignment parameters or their combination. The comparison of the residual artefacts after AAS is therefore not biased by differences in the level of movement at the two different positions.

The temporal SNR of the EPI data averaged over the ROI in visual cortex was not significantly different at the two positions, with the average over subjects taking values of 77 ± 21 at the 0 cm position and 86 ± 18 at the 4 cm position. A Wilcoxon signed-rank test on the individual subject data also showed no significant change in SNR with position.

Figure 6 shows a comparison of the anatomical images from one subject acquired with the nasion at iso-centre and then axially shifted by 4 cm to the optimal position. Three sagittal slices drawn from the 160-slice data sets acquired at the two positions are shown in Fig. 6A and B. There are no obvious discrepancies between the two sets of images. The corresponding difference images formed by: (i) subtracting the data acquired with and without the 4 cm shift, and (ii) by subtracting two different image data sets acquired with the subject's nasion at isocentre are shown in Figs. 6C and D. The deviations from zero are similar in the two difference images, indicating that there is no obvious effect of the 4 cm shift on the anatomical images. The differences that are seen in both data sets most likely result from small errors in co-registration and the variable effects of flow in the cerebro-spinal fluid and large blood vessels.

Discussion

The results of Study 2 show that it is possible to produce a significant reduction in the magnitude of the gradient artefacts which appear in EEG data recorded during concurrent fMRI (based on axial, multi-slice EPI) by axially repositioning the subject so that the nasion is shifted 4 cm from the scanner's iso-centre towards the feet (Figs. 3 and 4). The 40% reduction in the RMS value and the 31% reduction in the range of the artefact over electrodes that is produced by this shift are broadly consistent with changes in the amplitude of the voltages generated by gradient pulses applied on each of the three Cartesian axes that were measured in Study 1 (Fig. 2). The reduction in the magnitude of the gradient artefact means that simple repositioning of the subject will allow EEG data to be recorded with a larger bandwidth or a smaller dynamic range during concurrent fMRI, without saturating the amplifiers. Preliminary experiments carried out for Study 2 provided an illustration of this behaviour: we found that with a 1 kHz low-pass frequency cut-off, the occipital electrode channels were saturated during execution of the multi-slice EPI sequence when the subject's nasion was at iso-centre, but no saturation occurred when the subject was shifted axially by 4 cm (a 250 Hz cut-off frequency was therefore used for the actual study). The benefits of the reduction in artefact amplitude and consequent access to a higher bandwidth in recording are most likely to be realised in studying high frequency brain activity, such as gamma oscillations. Recently, for example, Freyer *et al* (Freyer et al. 2009) described a method for studying high frequency brain activity during simultaneous EEG-fMRI which involved opening up the bandwidth and then interpolating over data points sampled at times where the gradient artefact saturated the amplifiers. Use of the optimal positioning technique should reduce the amount of interpolation required, thus improving data quality.

Analysis of signals occurring at frequencies corresponding to the harmonics of the 12.8 Hz slice acquisition frequency (Fig. 5) in the EEG data that had been corrected using AAS showed that the residual gradient artefact was also significantly reduced (by 36%) by recording with the subject at the optimal axial position. The data used for this analysis were recorded in an experiment where small subject movements, with a cumulative magnitude of less than 1 mm, occurred during acquisition. Subject movements of this order of magnitude hamper the effectiveness of gradient artefact correction using AAS due to the sensitivity of the artefact morphology to head position (Moosmann et al. 2009) and the residual gradient artefacts that result can easily dominate the neuronal signals of interest. In this study, for example, the standard deviation across slice acquisitions of the residual artefact voltage averaged across subjects and leads peaked at a value of about 100 μV above baseline (occurring at time-points in the slice acquisition when the uncorrected artefact was largest) when the subjects were positioned with nasion at iso-centre (Fig. 4). The significant reduction in the residual artefact produced by axial repositioning is likely to provide a valuable increase in the signal to noise ratio of EEG data recorded during concurrent fMRI. This reduction may be of particular interest when considering oscillatory activity in the gamma band and above, since residual gradient artefacts are often found to be larger in this frequency range (Mullinger et al. 2008a), while oscillatory electrical activity is generally weaker in amplitude than that occurring at lower frequency (Orrison et al. 1995).

It is important to note that the reduction in the magnitude of the raw and residual gradient artefacts demonstrated here can be produced without compromising the quality of the MRI data used for both anatomical (see Fig. 6) and functional imaging (as indicated by the negligible change in the temporal SNR of the EPI data recorded in Study 2 after axial repositioning). This is to be expected since the optimal subject position is produced by shifting the subject by just 4 cm while the magnetic field homogeneity and gradient linearity are adequate for imaging over a 40 cm diameter spherical volume in the Philips Achieva 3 T scanner used in these experiments. A similarly large region of uniformity is provided by other scanner manufacturers. In fact the optimal position used here effectively centres the brain (rather than the entire head) at the scanner's iso-centre. When the +4 cm shift is adopted, the brain is therefore also optimally positioned for MRI.

The focus of the study described here is an experimental demonstration of the reduction of the magnitude of the gradient artefacts that can be produced by adjustment of the subject's axial position. This idea arose from previous work in which we calculated the amplitude and distribution of the gradient artefacts using simple analytical and numerical models wherein the contributions to the artefact from voltages induced in the leads and in a spherical volume conductor (which models the head) were combined (Yan et al. 2009). In particular, the analytic expressions for the artefacts generated by uniform, time-varying transverse and longitudinal gradients, based on lead paths following lines of longitude on the upper half of the spherical model head, showed that a reduction in artefact amplitude could be produced by shifting the sphere so that the scanner's iso-centre (where z = 0) lay between the centre and top of the sphere. A simple explanation for this reduction is that such an axial shift decreases the maximum magnetic field variation experienced by the leads and upper half of the sphere, since for each of the three gradients, one Cartesian component of the magnetic field varies linearly with z-position and is nulled when $z = 0$ (Yan et al. 2009). Similarly, reducing the maximum magnitude of the temporally-varying magnetic fields that the EEG leads and the relevant portion of the volume conductor are exposed to might be expected to decrease the variation in artefact voltage produced by small changes in position. The simple analysis thus provides some explanation for the reduction of the gradient artefact, measured before and after AAS, that was produced by axial repositioning in our experimental study. Since the gradient artefacts depends on the spatial variation of the applied magnetic field gradients over the head and leads (Yan et al. 2009) and are not dependent in any way on the

orientation or strength of the main static magnetic field, our findings are relevant to whole body scanners supplied by different manufacturers and to those operating at different field strengths (e.g. 1.5T). It is likely that the optimal position of the subject will depend to some extent on the wiring layout of the EEG cap used and also on the shape and size of the subject's head. However, analysing the data from Study 1 at the individual subject level we did find that the artefacts due to the different gradients were generally minimised at similar axial positions, suggesting that there is no great advantage in individually optimising the position of the subject.

There are, however, some aspects of the experimental results that are not readily explained by the simple analysis and require further discussion. In particular, the analysis in which the head is modelled as a sphere predicts that the artefacts produced by transverse (RL & AP) and longitudinal (FH) gradients would show a somewhat different dependence on axial position, as is seen in the experimental data, but also forecasts identical behaviour for the RL and AP gradients. The latter feature is not shown in the experimental data, wherein a shift of 4-6 cm minimises the RMS voltage induced by a time-varying RL gradient, while a shift of 0-2 cm produces the smallest effect for an AP gradient (Fig. 2). This discrepancy probably results in part from deviation of real head-shape from the model sphere. Caucasian heads generally have a significantly greater length (AP dimension) than width (RL dimension) and this lack of symmetry would be expected to change the relative sensitivity to gradients applied in the AP and RL directions. It is interesting to note that the artefact voltages due to the AP gradient also show the largest variation across subjects (as denoted by the error bars in Fig. 2), which might point towards a greater sensitivity of artefacts from this gradient to variation in head shape. However this isn't reflected in a dominant variation in the measured head size in the AP dimension (dAP). Our previous work also showed that significant voltages (~ 150 μV) are generated by the effect of the temporal varying gradients on the cable tree and ribbon cable that connect the EEG cap to the EEG amplifiers (Yan et al. 2009) and these voltages will interfere with those produced in the head and EEG leads. The effect of these voltages may also contribute to the difference in sensitivity to AP and RL gradients. Further work is needed to characterise the voltages due to the cable tree and ribbon cable and to identify the positioning of the cable and amplifier which best limits the size and variability of the gradient artefacts. In addition the effects of head shape on the artefacts could be further explored. This might lead to small adjustments in the optimal axial offset.

Conclusions

In conclusion, we found that positioning subjects so that their nasion was displaced 4 cm axially from the scanner's iso-centre towards the feet significantly reduces the gradient artefact produced by time-varying gradients applied in the RL and FH directions compared with the situation where the nasion is at iso-centre. Further measurements showed that this decrease translates into a 40% reduction in the RMS amplitude of the gradient artefacts generated during conventional multi-slice EPI acquisition as used in most EEG-fMRI experiments. This reduction in artefact amplitude provides the opportunity to record EEG data during concurrent fMRI with higher bandwidth without amplifier saturation. The optimised recording position also produced a 36% reduction in the residual gradient artefact after AAS has been applied to EEG data recorded from human subjects executing cued foot movements that produced changes in head position representative of a typical fMRI experiment. The optimal, 4 cm axial shift is small compared with the extent of the homogeneous region of a modern MR scanner and so does not compromise MR image quality. We recommend that this shifted subject position be adopted in all future EEG-fMRI studies.

Acknowledgments

KM and WY were supported by the University of Nottingham's Mansfield Fellowship scheme. We thank Mr Takayuki Ohma for assistance with the acquisition and preliminary analysis of some data shown here.

References

Allen PJ, Josephs O, Turner R. A Method for removing Imaging Artifact from Continuous EEG Recorded during Functional MRI. Neuroimage. 2000; 12(2):230–239. [PubMed: 10913328]

Allen PJ, Poizzi G, Krakow K, Fish DR, Lemieux L. Identification of EEG Events in the MR Scanner: The Problem of Pulse Artifact and a Method for Its Subtraction. Neuroimage. 1998; 8(3):229–239. [PubMed: 9758737]

Anami K, Mori T, Tanaka F, Kawagoe Y, Okamoto J, Yarita M, Ohnishi T, Yumoto M, Matsuda H, Saitoh O. Stepping stone sampling for retrieving artifact-free electoencephalogram during functional magnetic resonance imaging. Neuroimage. 2003; 19(2):281–295. [PubMed: 12814579]

Benar CG, Schon D, Grimault S, Nazarian B, Burle B, Roth M, Badier J-M, Marquis P, Liegeois-Chauvel C, Anton J-L. Single-Trial Analysis of Oddball Event-Related Potentials in Simultaneous EEG-fMRI. Human Brain Mapping. 2007; 28:602–613. [PubMed: 17295312]

Comi E, Annovazzi P, Silva AM, Cursi M, Blasi V, Cadioli M, Inuggi A, Falini A, Comi G, Leocani L. Visual Evoked Potentials May Be Recorded Simultaneously With fMRI Scanning: A Validation Study. Human Brain Mapping. 2005; 24:291–298. [PubMed: 15678479]

Debener S, Mullinger KJ, Niazy RK, Bowtell RW. Properties of the ballistocardiogram artefact as revealed by EEG recordings at 1.5, 3 and 7 Tesla static magnetic field strength. International Journal of Psychophysiology. 2008; 67(3):189–199. [PubMed: 17683819]

Debener S, Ullsperger M, Siegel M, Engel AK. Single-trial EEGfMRI reveals the dynamics of cognitive function. Trends in Cognitive Sciences. 2006; 10(12):558–563. [PubMed: 17074530]

Eichele T, Specht K, Moosmann M, Jongsma MLA, Quiroga RQ, Nordby H, Hugdahl K. Assessing the spatiotemporal evolution of neuronal activation with single-trial event-related potential and functional MRI. Proceedings Of The National Academy Of Sciences Of The United States Of America. 2005; 102(49):17789–17803.

Ertl M, Kirsch V, Leicht G, Karch S, Olbrich S, Reiser M, Hegerl U, Pogarell O, Mulert C. Avoiding the ballistocardiogram (BCG) artifact of EEG data acquired simultaneously with fMRI by pulse-triggered presentation of stimuli. Journal of Neuroscience Methods. 2010; 186:231–241. [PubMed: 19931564]

Freyer F, Becker R, Anami K, Curio G, Villringer A, Ritter P. Ultrahigh-frequency EEG during fMRI: Pushing the limits of imaging-artifact correction. Neuroimage. 2009; 48(1):94–108. [PubMed: 19539035]

Gebhardt H, Blecker CR, Bischoff M, Morgen K, Oschmann P, Vaiti D, Sammer G. Synchronized measurement of simultaneous EEG-fMRI: A simulation study. Clinical Neurophsiology. 2008; 119(12):2703–2711.

Iannetti GD, Di Bonaventura C, Pantano P, Giallonardo AT, Romanelli PL, Bozzao L, Manfredi M, Ricci GB. fMRI/EEG in paroxysmal activity elicited by elimination of central vision and fixation. Neurology. 2002; 58(6):976–979. [PubMed: 11914422]

Ives JR, Warach S, Schmitt F, Edelman RR, Schomer DL. Monitoring a patient's EEG during echo planar MRI. Electroencephalography and Clinical Neurophysiology. 1993; 87(6):417–420. [PubMed: 7508375]

Laufs H, Duncan JS. Electroencephalography/function MRI in human epilespy: what it currently can and cannot do. Current Opinion in Neurology. 2007; 20(4):417–423. [PubMed: 17620876]

Laufs H, Krakow K, Sterzer P, Eger E, Beyerle A, Salek-Haddadi A, Kleinschmidt A. Electroencephalographic signatures of attentional and cognitive default modes in spontaneous brain activity fluctuations at rest. Proceedings Of The National Academy Of Sciences Of The United States Of America. 2003; 100(19):11053–11058. [PubMed: 12958209]

Lemieux L. Electroencephalography-correlated functional MR imaging studies of epileptic activity. Neuroimaging Clinics of North America. 2004; 14(3):487. + [PubMed: 15324860]

Mandelkow H, Halder P, Boesiger P, Brandeis D. Synchronisation facilitates removal of MRI artefacts from concurrent EEG recordings and increases usable bandwidth. Neuroimage. 2006; 32(3):1120–1126. [PubMed: 16861010]

Mayhew S, Dirckx SG, Naizy RK, Iannetti GD, Wise RG. EEG signatures of audiotory activity correlate with simultaneously recorded fMRI responses in humans. Neuroimage. 2010; 49(1):849–864. [PubMed: 19591945]

Mobascher A, Brinkmeyer J, Warbrick T, Musso F, Wittsack HJ, Saleh A, Schnitzler A, Winterer G. Laser-evoked potential single-trial amplitudes covary with the fMRI BOLD response in the medial paon system and interconnected subcortical structures. Neuroimage. 2009; 45(3):917–926. [PubMed: 19166948]

Moosmann M, Schonfelder VH, Specht K, Scheeringa R, Nordby H, Hugdahl K. Realignment parameter-informed artefact correction for simultaneous EEG-fMRI recordings. Neuroimage. 2009; 45(4):1144–1150. [PubMed: 19349230]

Mugler JP, Brookeman JR. 3-Dimensional Magnetization-Prepared Rapid Gradient-Echo Imaging (3dmp-Rage). Magnetic Resonance In Medicine. 1990; 15(1):152–157. [PubMed: 2374495]

Mullinger KJ, Morgan PS, Bowtell R. Improved Artefact Correction for Combined Electroencephalography/Functional MRI by means of Synchronization and use of VCG Recordings. Journal of Magnetic Resonance Imaging. 2008a; 27(3):607–616. [PubMed: 18307200]

Mullinger, KJ.; Brookes, MJ.; Geirsdottir, GB.; Bowtell, R. Human Brain Mapping. Elsevier; Melbourne: 2008b. Average Gradient Artefact Subtraction: the effect on neuronal signals.

Mullinger KJ, Brookes MJ, Stevenson CM, Morgan PS, Bowtell R. Exploring the feasibility of simultaneous EEG/fMRI at 7T. Magnetic Resonance Imaging. 2008c; 26(7):607–616.

Orrison, WW., Jr; Lewine, JD.; Sanders, JA.; Hartshorne, MF. Functional Brain Imaging; Chapter 8: Clinical Electroencephalography and Event-Related Potentials. Mosby; St Louis: 1995.

Ryali S, Glover GH, Chang C, Menon V. Development, validation, and comparison of ICA-based gradient artifact reduction algoithms for simultaneous EEG-spiral in/out and echo-planar fMRI recordings. Neuroimage. 2009; 48(2):348–361. [PubMed: 19580873]

Salek-Haddadi A, Friston KJ, Lemieux L, Fish DR. Simultaneous EEG-Correlated Ictal fMRI. Neuroimage. 2002; 16:32–40. [PubMed: 11969315]

Salek-Haddadi A, Friston KJ, Lemieux L, Fish DR. Review: Studying spontaneous EEG activity with fMRI. Brain Research Reviews. 2003; 43:110–133. [PubMed: 14499465]

Schubert R, Ritter P, Wustenberg T, Preuschhof C, Curio G, Sommer W, Villringer A. Spatial attention related SEP amplitude modulations covary with BOLD signal in S1-a simultaneous EEG-fMRI study. Cerebral Cortex. 2008; 18(11):2686–2700. [PubMed: 18372293]

Strobel A, Debener S, Sorger B, Peters JC, Kranczoich C, Hoechstetter K, Engel AK, Brocke B, Goebel R. Novelty and target processing during an auditory novelty oddball: a simultaneous event-related potential and functional magnetic resonance imaging study. Neuroimage. 2008; 40(2):869–883. [PubMed: 18206391]

Warbrick T, Mobascher A, Brinkmeyer J, Musso F, Richter N, Stoecher T, Fink GR, Shah NJ, Winterer G. Single trial P3 amplitude and latency informed event related fMRI models yield different BOLD response patterns to a target detection task. Neuroimage. 2009; 47(4):1532–1544. [PubMed: 19505583]

Yan WX, Mullinger KJ, Brookes MJ, Bowtell R. Understanding Gradient Artefacts in Simultaneous EEG/fMRI. Neuroimage. 2009; 46(2):459–471. [PubMed: 19385014]

Yan WX, Mullinger KJ, Geirsdottir GB, Bowtell R. Physical Modelling of pulse artefact sources in simultaneous EEG/fMRI. Human Brain Mapping. 2010; 31(4):604–620. [PubMed: 19823981]

Europe PMC Funders Author Manuscripts

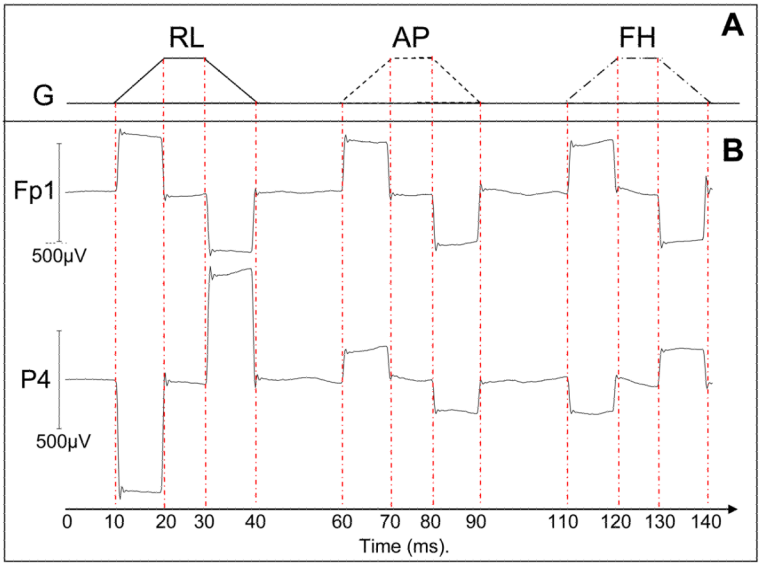

Figure 1.
Illustration of the sequence used to characterise the artefacts generated by time-varying gradients along each Cartesian axis. **(A)** Schematic illustration of the gradient pulses applied in the right-left (RL), anterior-posterior (AP) and foot-head (FH) directions; (**B**) Average artefact voltages generated by these pulses on two example leads (FP1 and P4).

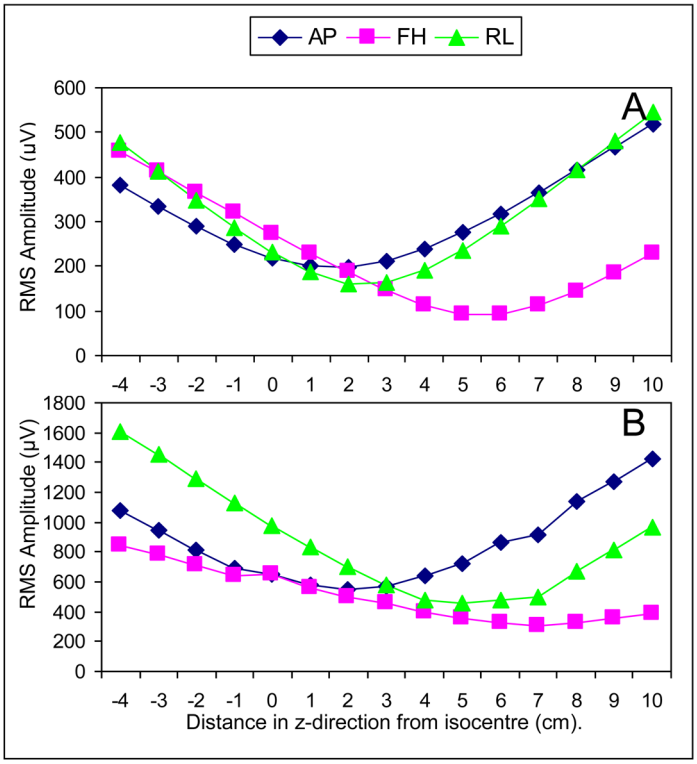

Figure 2.
Variation of the average gradient artefact (RMS value (**A**) and range (**B**) over electrodes) with subject's axial position for gradients applied in RL, FH & AP directions (0 cm = nasion at iso-centre). Error bars show standard deviation across the six subjects studied.

Europe PMC Funders Author Manuscripts

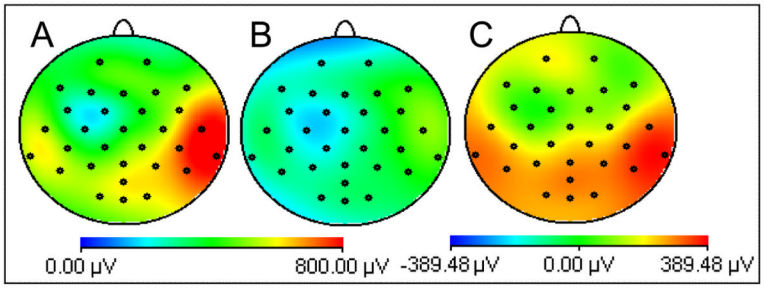

Figure 3.
Maps of the RMS (over time) of the gradient artefact produced by a multi-slice EPI acquisition with the nasion at: **A**) iso-centre; **B**) +4 cm. **C**) shows the difference, **A**-**B**. Data averaged over six subjects.

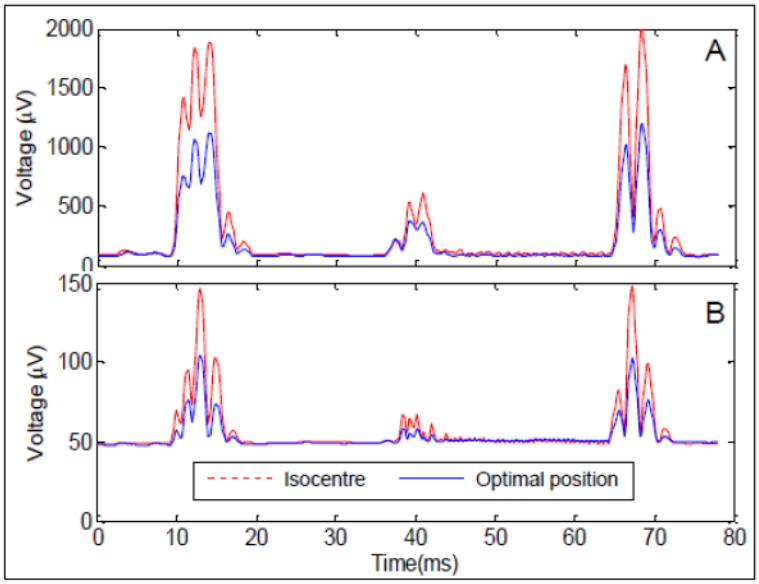

Figure 4.

A: The RMS over channels of the average slice artefact before artefact correction averaged across subjects at the iso-centre (red dashed line) and optimal position (blue line). **B:** The standard deviation across slices after artefact correction using AAS averaged across subjects at the iso-centre (red dashed line) and optimal position (blue line). Only data acquired during time periods when the subject was stationary were used here.

Europe PMC Funders Author Manuscripts

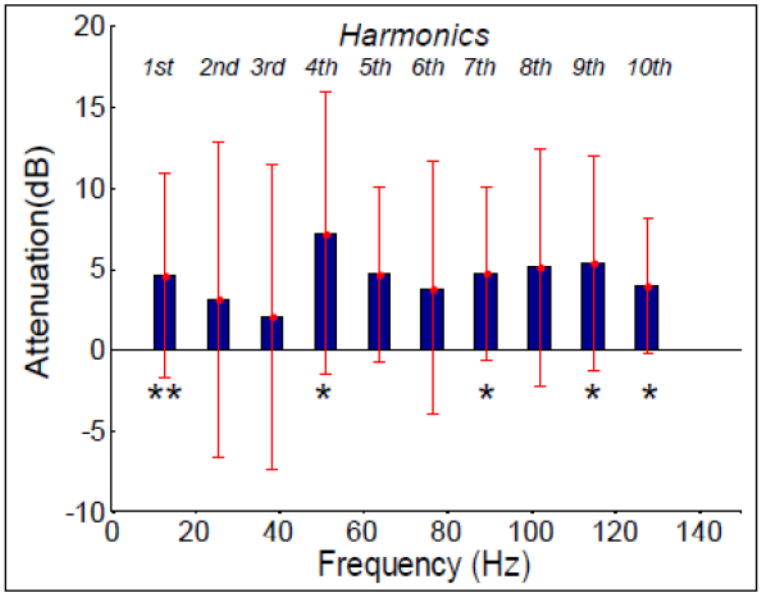

Figure 5.

Attenuation of signal power at optimal position compared to iso-centre after gradient artefact correction for first ten harmonics of the slice frequency, averaged over channels and subjects. Error bars: standard deviation over subjects. Asterisks indicate where a significant reduction was found: ** denotes $p< 0.05$ and * denotes $p<0.1$.

Europe PMC Funders Author Manuscripts

Europe PMC Funders Author Manuscripts

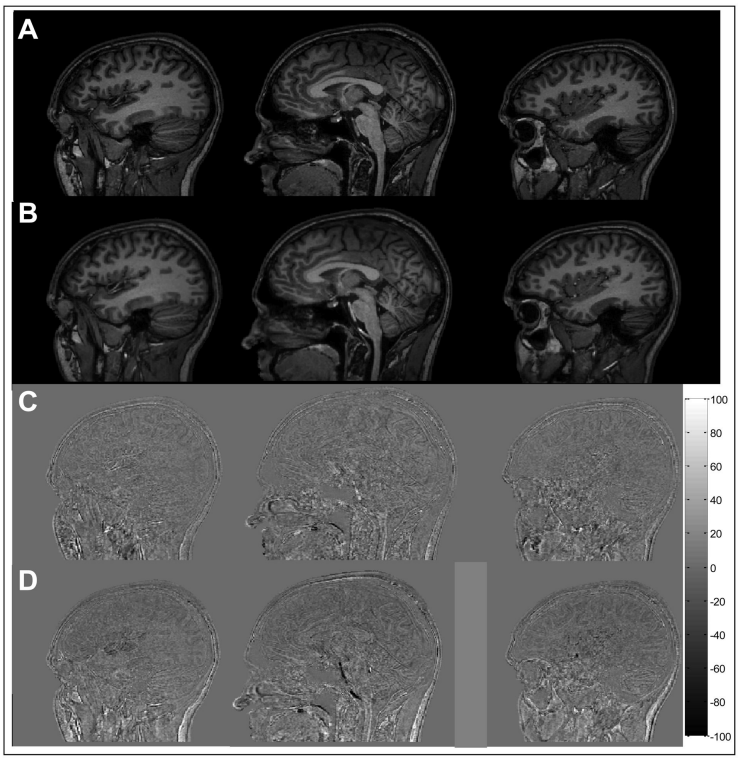

Figure 6.
Standard anatomical image acquired at: **A**) iso-centre, **B**) +4 cm. **C)** shows the difference of two images acquired at iso-centre and **D**) shows the difference of **A** and **B**. In both cases the images were co-registered before subtraction. The colour bar shows the relationship of grey-scale to the percentage of the mean of the original images acquired at iso-centre.